International Journal of Latest Engineering Research and Applications (IJLERA) ISSN: 2455-7137

Volume – 04, Issue – 01, January 2019, PP – 01-11

Study of the stability margin and its connection with the dynamic stiffness applied to a tidal turbine

B. Fraga De Cal

Mechanical Engineer MSc. (Nebrija University, Spain)
Renewable Energy, MSc. (Queen Mary University of London)
Mechanical Engineer Designer, Energy & Sustainability
Ph D. Student, A Coruña University, Spain

Abstract: In a rotary machine, when a fluid, liquid or gas is present, located in the space between the rotor and its static part, two concentric cylinders, the fluid moves in that clearance tangentially. The forces that create the pressurized fluid are perpendicular to the surface of the static component, which can cause the so-called phenomena whirl and whip at its natural frequency.

The test that is exposed is applied to the sealing seal of a tidal turbine, which has a pressurized lubrication to prevent water from entering the machine. It is revealed that the "stability margin" of a rotor decreases when the rotor speed approaches the "stability threshold", so that the rotor approaches an unstable operating range. The "Dynamic Stiffness" becomes zero at the frequency of the whirl and whip. It is also noted that a rotor operating in a fluid instability presents values of zero of the Direct and Quadrature Dynamic Stiffness in the same frequency.

A stable operation of the rotor will occur at the speed limits defined by the stability margin. In this way, you must pre-calculate the limits of that margin, so that if the marine currents drive to turn the rotor out of those limits, the turbine must be stopped so as not to cause serious breakdowns. The method for that calculation is presented, in this work.

Keywords: Tidal Turbines; Rotor dynamics; whirl & whip; dynamic stiffness; stability margin.

1. Introduction

The concern for stable operation and the life of the tidal turbines is constant and current, as demonstrated by the MARINET 2 (EU) project, for example, and one of its latest researches (Ordonez, Porter, & Allmark, 2018). Wave loading on tidal turbines is of key concern for determining blade and drive train design loads and the fatigue life of components.

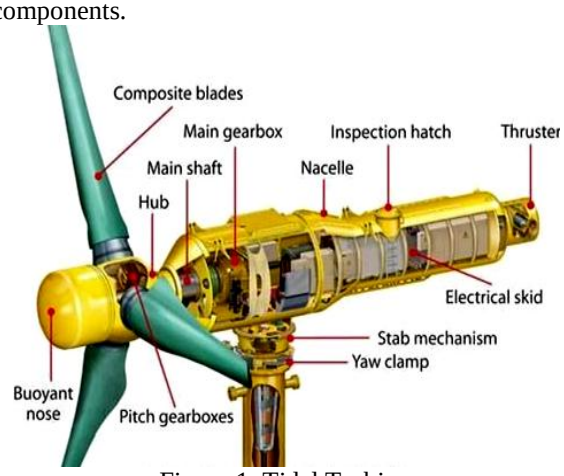

Figure 1. Tidal Turbine

The sealing seal is a fundamental part of the tidal turbines (Figure 1), since it not only acts as a bearing but must prevent the entry of seawater into the machine. It has, normally, several sealing gaskets in addition to a pressurized oil environment to lubricate the shaft and keep the seal safe. This environment is maintained with pressurized oil at 0,3 bars above the value of the outside (Figure **2**).

Although the hydrostatic bearing or seal was invented in 1862 by L. Girard, it seems to have been avoided as a means of stabilizing the rotor systems. For many years, the lubrication theory has pointed out that a fully lubricated cylindrical rotor is unstable. Newirk and Kimball introduced the oil wedge pressure

modification to provide a static charge to the rotor to decrease instability. This situation is the one that occurs in the pressurized oil environment of the sealing seal.

The asymmetric clearance caused by the eccentric operation as is the case of the sealing seal cause the fluid to generate a support force in the periphery of the stator representing the circumferential forces of the flow.

The average angular velocity of this flow is a fraction of the rotary speed of the rotor (Ω) which is called the "circumferential average velocity ratio of the fluid" (λ). The velocity of the fluid on the surface of the static part is zero while on the surface of the shaft is equal to the speed of the rotor, so that the circumferential average velocity of the fluid in the shaft/seal gap can be expressed as "ΛΩ" (Childs D., 1993). The value of λ is usually somewhat less than ½.

This force can be parted in a tangential force perpendicular to the radial displacement of the rotor, in the direction of the flow of the fluid, and a radial that points towards the center of the seal, according to Figure 3. Both, radial and tangential forces are proportional to the displacement of the shaft from the center of the seal. Thus, the lubricating fluid act as a spring with a *complex stiffness*, the radial of the stiffness of the fluid wedge is considered as the *spring stiffness* and the tangential part as *tangential stiffness*. This fluid spring operation provides shaft support.

If the shaft moves from the equilibrium position, the tangential force pushes the shaft in the tangential direction, and the stiffness force of the spring attempts to return this shaft to the original position. In fact, the instability of the fluid is caused by the relationship between the stiffness of the spring, the inertia of the rotor (which produces the mass), the damping force and the tangential stiffness (Bently & Hatch, 1993), (Muszynska & Yu, 2005).

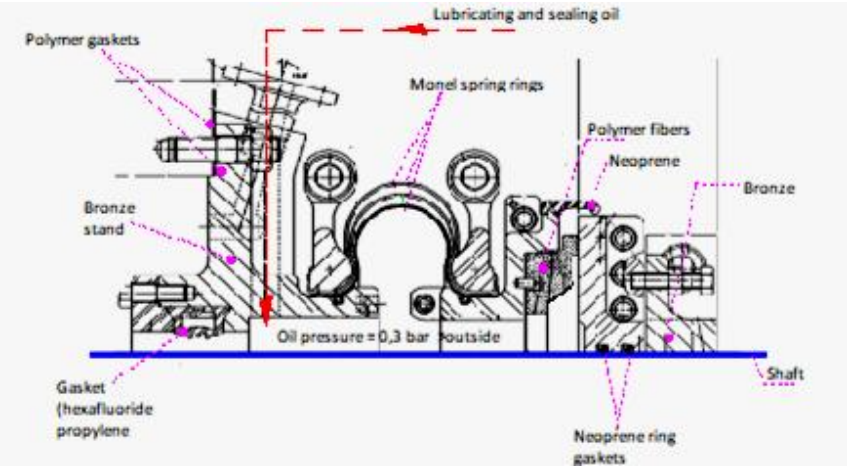

Figure 2. Sealing seal

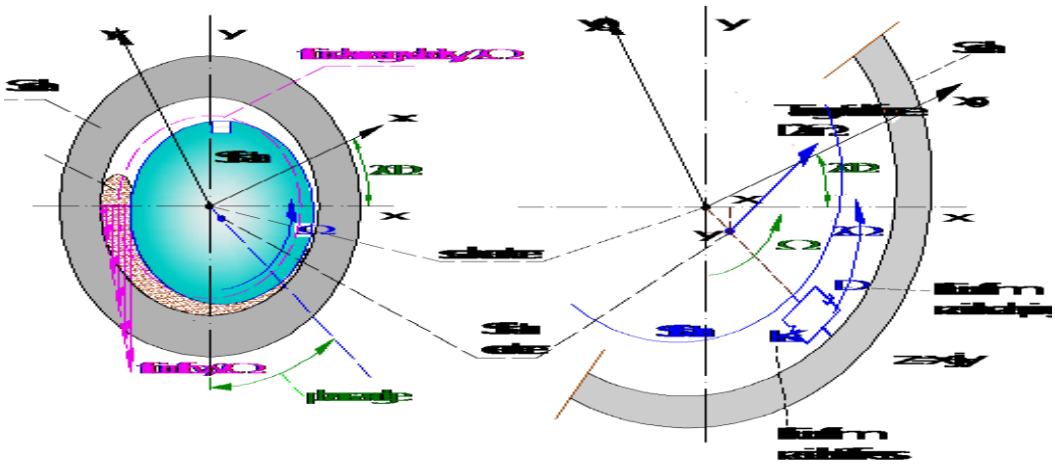

Figure 3. Fluid film for shaft rotating

For a symmetrical rotor supported on a fluid-lubricated bearing or seal, the mathematical model of the movement is as follows:

$$M\ddot{z} + M_{fl}(\ddot{z} - 2j\lambda\Omega\dot{z} - \lambda^2\Omega^2 z) + D(\dot{z} - j\lambda\Omega z) + Kz + K_B z = Fe^{j\omega t} \qquad [1]$$

$$z = x + jy \qquad j = \sqrt{-1}$$

where M, K are rotor mass and stiffness respectively; M_f, D, K_B are fluid inertia, radial damping and radial stiffness, respectively; Ω is the rotating speed; λ is the speed coefficient of fluid; ω is perturbation frequency; the variable z(t) represents the radial displacement of the shaft (horizontal "x" and vertical "y").

The vibration is simply the answer to a disturbance conditions in a machine. It is the relation of the forces acting on the machine and its stiffness:

$$Vibration\ (Response)\ \vec{R} = \frac{Force\ \vec{F}}{Dynamic\ Stiffness\ (Restraint)\vec{K}_{DS}}$$

The rotor system Dynamic Stiffness is as follows (Tam, Przekwas, Hendricks, & Braun, 1988):

$$\vec{K}_{DS} = [K - M\Omega^2] + j\,[D(1-\lambda)\Omega]$$

A synchronous excitation force can be an imbalance of mass in the rotor; this means that the force of the inlet has the same frequency as the speed of the rotor. This imbalance causes a centrifugal force: $\vec{F} = \overrightarrow{(mr_u\Omega^2)\angle\delta}$; m, unbalance mass; r_u unbalance radius; Ω rotative speed and δ phase lag of the unbalance mass:

$$\vec{R} = \frac{\overrightarrow{(mr_u\Omega^2)\angle\delta}}{\overrightarrow{[K - M\Omega^2] + j\,[D(1-\lambda)\Omega]}} \qquad [2]$$

In classical rotor dynamics for laterally isotropic systems, the seal fluid film *Direct Dynamic Stiffness* (K_D) and the *Quadrature Dynamic Stiffness* (K_Q) are:

$$K_D = K - M\Omega^2 \quad ; \quad K_Q = [D(1-\lambda)\Omega]$$

The *direct dynamic stiffness* according to the frequency "ω" is a parabola and the *quadrature dynamic stiffness* according to the frequency "ω" is a straight line that crosses the vertical axis on its negative side. The Dynamic Stiffness is a function of the excitation frequency and it is useful to see how Dynamic Stiffness changes as a result of perturbation frequency (Jang, Park, Kim, & Muszyinska, 1996).

2. Experimental Setup

The tested rotor model is in Figure 4. The disc mass of the rotor was placed about 6 cm from the bearing which is 10 cm from the lubricated seal with liquid, with a distance between the bearings of 53, 9 cm.

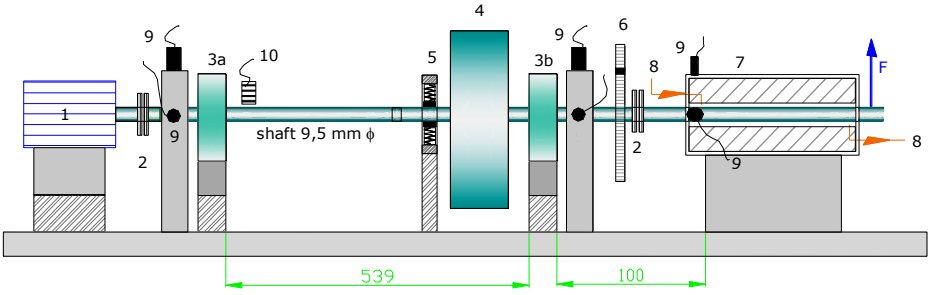

1: electric motor 0,1 HP; 2: Flexible coupling; 3a, 3b: bearing; 4: rotor mass 1,60 kg; 5: spring frame; 6: unbalanced disc; 7: oil lubricate seal; 8: oil circuit; 9: transducer, horiz.&vert.; 10: phase reference.

Figure 4. Experiment setup. Model rotor system

The rotor was driven by a 1/10 HP electric motor with a variable speed controller up to 5.000 rpm. A spring frame is installed to compensate for the gravity load on the rotor and center the shaft on the seal. The pressurized oil fluid is supplied through four radial points at a pump outlet pressure of 14 kPa. The oil temperature in a holding tank was 27 º C.

The test is as follows:

1) A known synchronous force, the centrifugal force generated by a calibration weight, is introduced.

2) The change in the synchronous response is then measured because of that force.

3) If the synchronous force and the response are known, according to equation [**2**], we can calculate the Synchronous Dynamic Stiffness, whose usefulness is very important:

- The tendency of dynamic stiffness provides valuable information about changes in machine parameters (mass, stiffness, damping).
- Dynamic Stiffness can be used to estimate the dynamic forces acting on a machine, such as those that cause a shaft/seal rubbing or a crack in the shaft.

3. Measure of Synchronous Dynamic Stiffness

There are five steps involved in determining dynamic stiffness:

1) Add a known imbalance mass to a known location and get response.
2) Measure the response due to the calibration weight only.
3) Measure the applied force of this imbalance mass.
4) Measure the synchronous dynamic stiffness.

I. Obtain data from startup and shutdown.

A point is selected, at 50 rpm, which is an own velocity of the rotor shaft driven by the sea currents of a tidal turbine. The response obtained is 2,75 mils ∠ 205º (R_1), according to Figure 5, and converted from polar to rectangular coordinates: -2,492 - j1,162 mil pp. No resonance frequency is observed until the speed of 800 rpm is surpassed.

II. Attach a known unbalance weight in a know location and get new data.

Add 1,25 gr. In a position of 90° at a radial distance of 105 mm. Its response is obtained at the same previous speed of 50 rpm with a vibration amplitude of 3,65 mils in the direction of 260 °, according to the diagram polar a) of Figure 6.

This new response is the sum of the first reference response of the rotor, in its original state without any disturbance (R_1) plus the weight of imbalance (R_2) that has been added.

The response is now R_1+R_2 = 3,65 mils∠260º (Figure **6**, polar diagram b)), which in rectangular form is: 1,858-j2,433. The response that is interesting to calculate is that which is due exclusively to the weight of the added imbalance R_3, and is carried out according to the graphic representation in polar of the Figure **7**.

	polar	Rectangular
$R_1 + R_2 =$	4∠210º mil pp	-0,634-j3,595
$- R_1 =$	2,75∠205º mil pp	-2,492 -j1,162
$R_3 =$	3,06∠307º mil pp	+1,858- j2,433

R_3 = 3,06 mil pp∠307º is the change in the response of the rotor system due to the added weight. In the Figure 7, R_3 moves to the origin of the polar diagram, in order to be able to easily observe the amplitude and the phase.

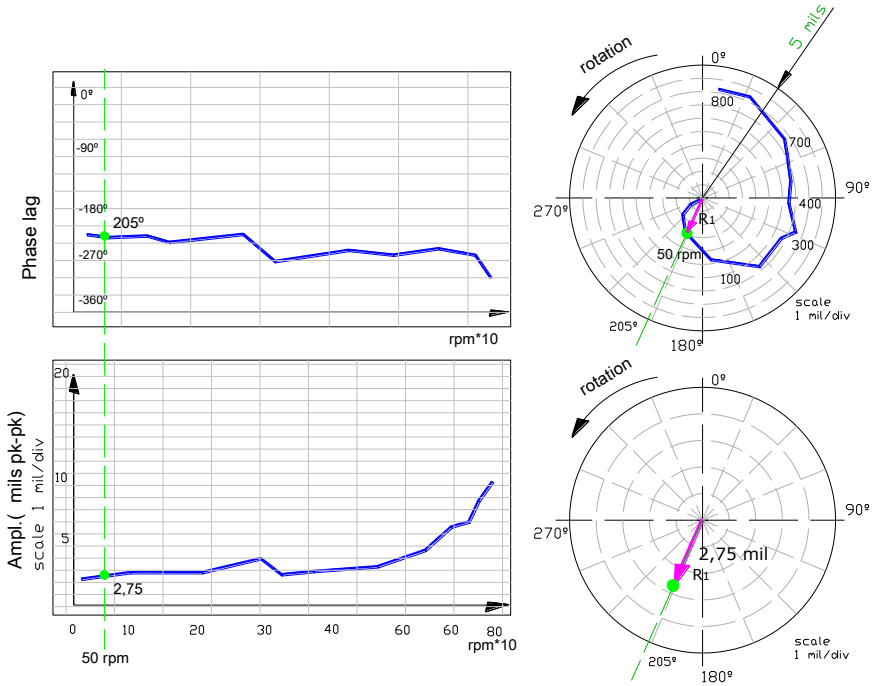

Figure 5. Data from startup. Bodé and polar plot.

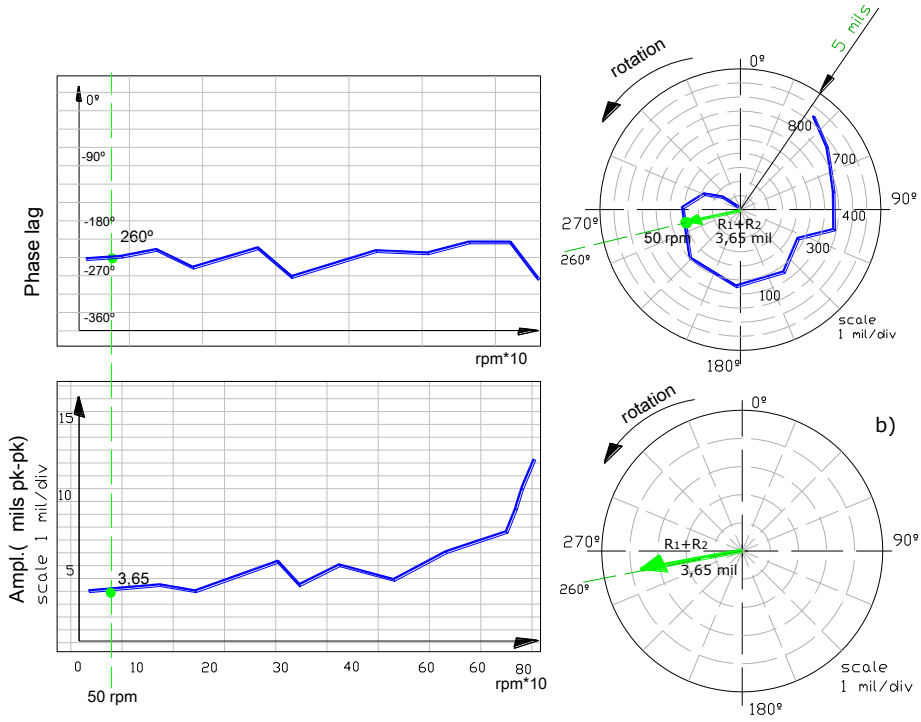

Figure 6. Data obtained with the known unbalanced weight.

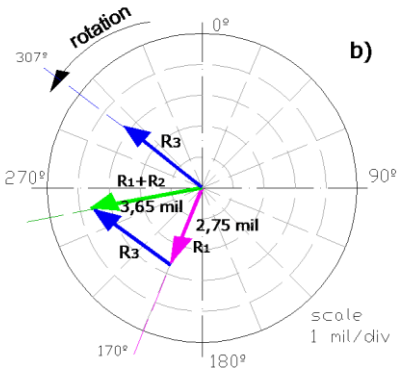

Figure 7. Response vector due to calibration only.

III. Calculate applied force from the calibration weight.

$\vec{F} = mr_u\Omega^2 e^{j\,\delta} = (1{,}25 * 10^{-3} kg)(105 * 10^{-3}\, m)\left[50\, rpm * \left(2\pi\, rad/_{1\, rev}\right)\left(1\, min/_{60\, sec}\right)\right]^2 \angle 90$

$= 3{,}59 * 10^{-3}\, N \angle 90^o$ p.p.

IV. Calculate Synchronous Dynamic Stiffness.

Dynamic stiffness is a zero-to-peak signal (N/m), so first the vibration amplitude of the response vector $(\overrightarrow{R_3})$ must be converted from peak to peak, to zero to peak (i.e. divide by 2):

$\vec{R}_3 =$ 3,06 / 2 ∠ 307º = 1,53 mils ∠ 269º = 0.0389*10^{-3} m. ∠ 307º

This response R_3, represented in a polar diagram as in Figure **7**, easily indicates its amplitude and phase. It is transferred to the vector field and matches the result of$(\vec{R}_1 + \vec{R}_2) - \vec{R}_1 = \vec{R}_3$.

$\vec{R}_3$ can be expressed as $\overrightarrow{R}_3 = Ae^{j\alpha}$, where "A" is the amplitude of the response and "α" the phase angle. The disturbing force of the controlled imbalance is: $\vec{F} = Fe^{j\delta}$:

$$\vec{K}_{DS} = \frac{\vec{F}}{\vec{R}} = \frac{F\, e^{j\,\delta}}{A\, e^{j\alpha}} = \frac{F}{A}\, e^{j\,(\delta-\alpha)} = \frac{F}{A} \angle(\delta-\alpha) = \frac{F}{R_3} \angle(\delta-\alpha)^o =$$

$$= \frac{3{,}59 * 10^{-3}}{0{,}0389 * 10^{-3}} \frac{N}{m} \angle(307-90) = 92{,}28\ {}^{\mathrm{N}}/_{\mathrm{m}} \angle 217^o$$

- Direct Dynamic Stiffness:

$K_D = K_{DS} * \cos\theta_k$ = 92,28 (N/m) *cos217º = -89,00 N/m

- Quadrature Dynamic Stiffness:

$K_Q = K_{DS} * \sin\theta_k$ = 92,28 (N/m) *sin217º = -24.35 N/m

This pre-test is performed with the same imbalance weight 1,25 gr. ∠90º, but at different rotation speeds, and the response data are taken to obtain these components of the dynamic stiffness depending on the rotation speed (Figure **8**).

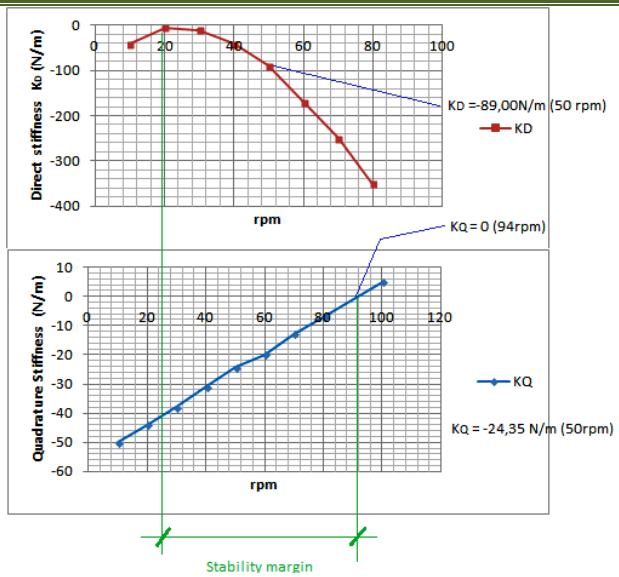

Figure 8. Calculating Synchronous Dynamic Stiffness over entire speed range

These calculations are shown in the graphs of Figure 8, a parabola for the real dynamic stiffness $K_D \angle \Omega^2$, and a straight line for the imaginary component $K_Q \angle \Omega$. This figure shows the values of the calculation example, for the speed of 50 rpm. The resonance value corresponds when in the actual component $Z_D = 0$, which occurs when $K\text{-}M\Omega^2 = 0$ and $\Omega = \sqrt{(K/M)}$, in this case no resonance is shown at the rpm margin studied, from 0 to 100 rpm.

The approximate value of the rotor spring coefficient is also indicated, extending the curve of the parabola to the intercession with the axis of the ordinate, where $\Omega = 0$, K = -90 N/m. For the Z_Q imaginary component graph, it becomes null when $JD\Omega = 0$, at 94 rpm.

In a stable system, the real and imaginary components of the dynamic stiffness are not zero at the same frequency. The "stability margin" is defined as the interval between the two null values (Sorge, 2016) which is where both Z_D as Z_Q have positive values. In the case analyzed is assumed from the inflection point of the parabola Z_D to the null value of the imaginary component = 94-18 = 76 rpm (Figure 8).

If both, Direct Dynamic Stiffness and Quadrature Dynamic Stiffness become zero at the same frequency, the denominator of equation [2] is made zero. There is nothing then that restrains the amplitude of vibration and the response tends to infinite. This is what happens at the *Threshold Stability*, when the rotor speed starts into fluid instability and it begins the so-called "whirling" phenomenon to later reach the "whip".

4. The experiment Results

With the purpose of investigating the Dynamic Stiffness of the rotor when operating in whirl and whip, it is necessary to apply a asynchronous perturbation on the rotor system operated at a constant speed (Force "F" in Figure **4**).

This disturbance is carried out near the fluid-lubricated seal by a constant rotating force of 0,15 kg at a variable rotation frequency. This disturbance is done with a flexible drive belt, thus isolating the belt loads from the rotor shaft. In addition, the spring frame ("5" in Figure 4) was adjusted to position the center of the shaft in the center of the seal.

Before calculating the dynamic stiffness experiment, the starting data were obtained from the rotor test platform and the Threshold Stability was observed about 105 rpm, so that the rotor becomes unstable at 105rpm in whirl and the transition to whip appears about 150 rpm, according Figure **9** (Che-Chao, Jhe-Wei, & Wen-Chang, 2011).

Therefore, to analyze the modifications of the S*tability Margin* in the stable zone and in the whirl and whip, the rotor was operated at 70 rpm (in the stable region), at the edge of fluid instability, 100 rpm (in whirl) and 150 rpm (in whip), subjected to the perturbation force (F in the Figure **4**).

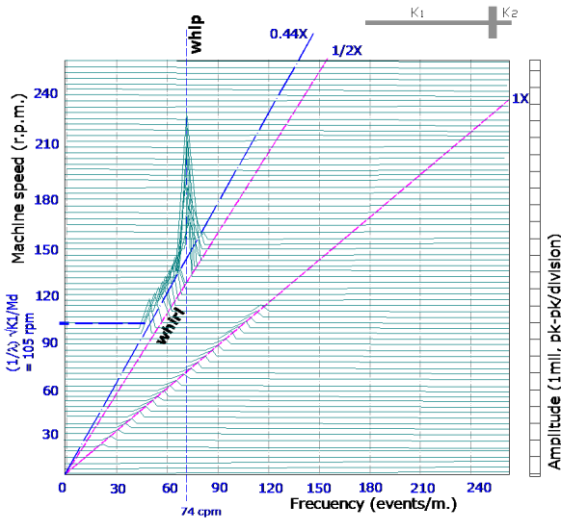

Figure 9. Start up. Cascade spectrum

The vibration data is acquired from vertical and horizontal induction current transducers placed on the fluid seal (9 in Figure 4), which are processed in a computer program of automated diagnostics for rotating equipment and filtered to the perturbation frequency (General Electric/Bently Nevada ADRE-208 Data Acquisition). The Dynamic Stiffness is calculated for each speed and in each run by the following expression, in accordance with the section 4).

$$\vec{K}_{DS} = \frac{\vec{F}}{\vec{R}}$$

where $\vec{F}$ *and* $\vec{R}$ are the perturbation force and filtered response of rotor, respectively.

The experimental data of Direct Dynamic Stiffness have the shape of a parabolic curve, and the Quadrature Dynamic Stiffness a straight line.

These results are shown in Figure **10** to Figure 12, in the stable zone. Figure **10** and Figure **11**, was obtained the Dynamic Stiffness while the rotor was running at 70 and 100 rpm, and was subjected to the described force that drives the belt.

It can be observed in the Figure **7** that the frequency separation between Direct and Quadrature Dynamic Stiffness, when both are made zero, is about 74 cpm and this value represents the *Margin of Stability*, for this case, while in Figure 10 that margin of stability is reduced to 40 cpm, and in Figure 11 at the rotation speed of 100 rpm, very close to the phenomenon of "whirl", is reduced to approximately 10 cpm.

These graphs show that when the rotor speed begins to approach the stability threshold (105 rpm), the stability range decreases.

The fluid-induced instability will appear when both the Direct and Quadrature Dynamic Stiffness are zero at the same frequency (Ugliara Mendes & Lucchesi Cavalca, 2014), A non-zero "Stability Margin" indicates that the rotor is not subject to fluid-induced instability at that speed range. When the rotor speed was increased to 100 rpm, where the "whirl" phenomenon started, the Direct and Quadrature Dynamic Stiffness approaches the value of zero at the same frequency, which is the whirl frequency of approximately 2600 cpm (Figure **11**), thus the *Stability Margin* becomes null also.

During this operation, the lubricating fluid ceases to work as a "wedge" on the seal and a completely lubricated shaft/seal gap occurs, a situation that does not produce stability, since the hydraulic forces of the fluid that hold the shaft disappear.

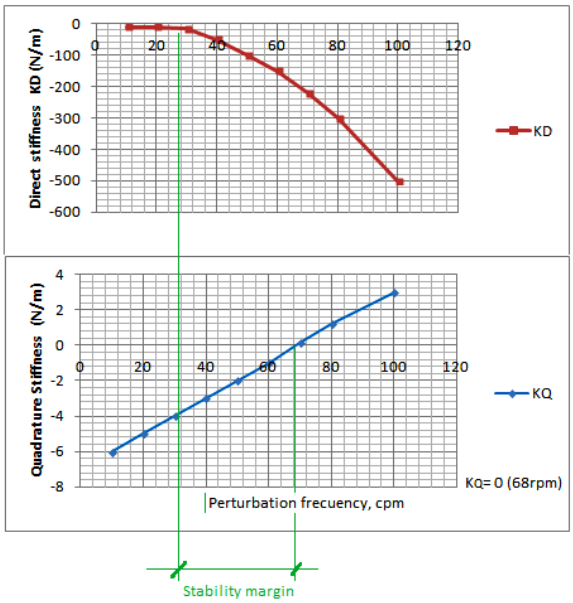

Figure 10. Dynamic Stiffness with rotor operating at 70 rpm in stable operation

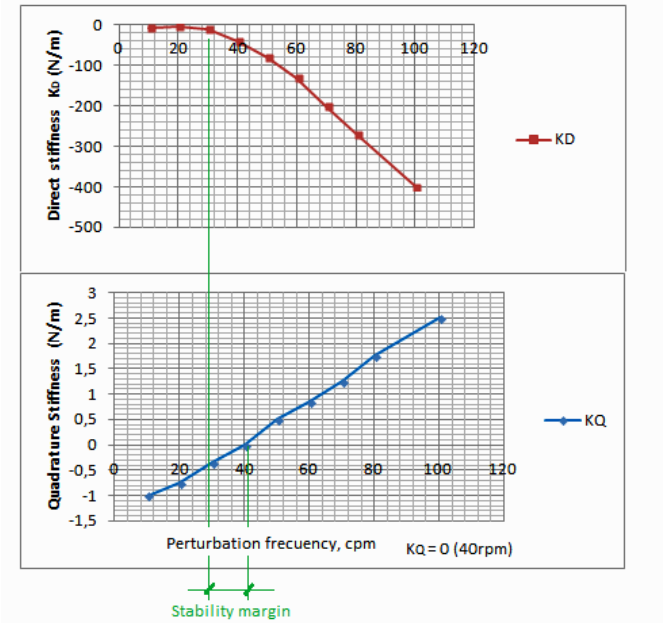

Figure 11. Dynamic Stiffness with rotor operating at 100 rpm, close "whirl"

On the other hand, as the speed of the rotor increased to 150 rpm, the phenomenon of "whip" starts and the graphs obtained correspond to the Figure 12, in which it can be observed that just like the "whirl", the Margin of Stability is zero and the Direct and Quadrature Stiffness become zero at the same frequency, 150 cpm ("whip" frequency).

The behaviour of the system no longer conforms to the simple rotor model that was used before, so it is not possible to achieve a form of standard curves, parabola for the real component and a straight line for the imaginary component, as the previous cases.

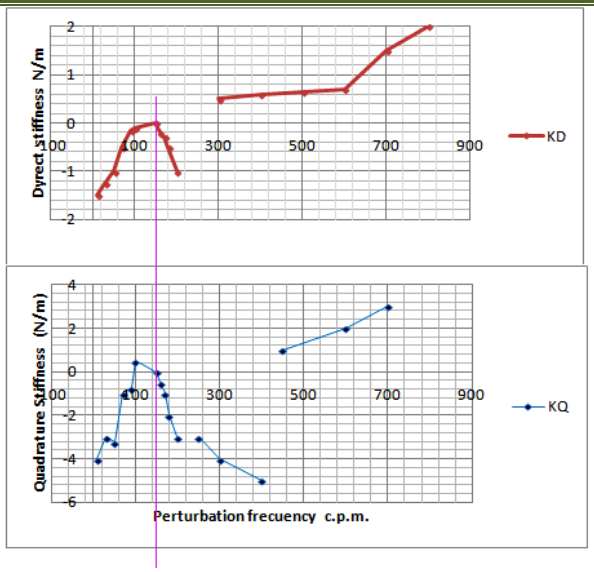

Figure 12. Dynamics Stiffness, oil whip at 150 rpm

Figure 13. Atlantis 2.0 MW Tidal Turbine

5. Conclusions

In these tests it is observed that the stability margin decreases as the rotor speed approaches the *Threshold Stability* that is where the phenomenon of whirl and whip begins in its natural frequency.

These results indicate that when the rotor is working near the whirl phenomenon and the whip, the S*tability Margin* is made zero and the direct dynamic rigidity and quadrature are also converted to zero at the same frequency.

For the whip data, the graphical results of *dynamic stiffness* cannot be easily obtained, the rotor's vibration would greatly increase in amplitude.

A stable operation of the rotor will always occur at operating speeds in the range that is defined by the margin of stability.

It is therefore essential to know these parameters of a system, in order to achieve the stability of the rotation to the possible instabilities of a shaft with lubricating fluid and watertight as is the case of the tidal turbine.

These limits of stability must be established so that according to the rotor speed which propels the marine currents, act on the braking system and thus avoid the production of strong vibrations. This essay has to be made in manufacturing, so that rotors like the Figure 13 that produce already 2MW not reach this problem.

6. Bibliography

[1]. S. Ordonez, K. Porter y M. Allmark, «Laboratory Study of Tidal Turbine Performance in Irregular Waves,» de *4th Asian Wave and Tidal Energy Conference*, Taipei, 2018.

[2]. Childs D., "Turbomachinery Rotordynamics," in *Jhon Wiley&Sons Inc.*, New York, 1993.

[3]. D. Bently y C. Hatch, «Root Locus and the Analysis of Rotor Stability Problems,» *Orbit, Bently Nevada Corporation*, vol. 14, nº 4, 1993.

[4]. A. Muszynska y J. Yu, «Effects of damping and Firiction on the rotor/seal or retaining bearing full annular rub,» de *Proceedings of the Third International Symposium on Stability Control of Rotating Machinery (ISCORMA-3)*, Cleveland, OH, USA., 2005.

[5]. L. Tam, A. Przekwas, R. Hendricks y M. Braun, «Numerical and Analytical Study of Fluid Dynamic Forces in Seals and Bearings.,» *Journal of Vibration, Acoustics, Stress, and Reliability en Design. Trans of the ASME.*, vol. 110, nº 3, pp. 315-325, 1988.

[6]. E. Jang, Y. Park, C. Kim y A. Muszyinska, «Identification of the quadrature resonances using modal nonsynchronous perturbation testing and dynamic stiffness approach for an anisotropic rotor system with fluid interaction,» *International Journal of Rotating Machinery*, vol. 2, nº 3, pp. 187-199, 1996.

[7]. F. Sorge, «Preventing the oil film instability in rotor-dynamics,» *Journal of Physics. Conference Series 744(1):012153*, 2016.

[8]. F. Che-Chao, S. Jhe-Wei y T. Wen-Chang, «Study of start-up vibration response for oil whirl and oil whip,» *Mechanical Systems and Signal Processing. DOI10.1016/j.ymssp.2011.04.012*, vol. 25, nº 8, pp. 3102-3115, 2011.

[9]. R. Ugliara Mendes y K. Lucchesi Cavalca, «On the Instability Threshold of Journal Bearing Supported Rotors,» *International Journal of Rotating Machinery. DOI-10.1155/2014/351261*, vol. 2014, nº February 2014, p. ID 351261, 2014.

[10]. D. Bently y S. Zimmer, «Interpreting vibration information from rotating machinery.,» *Transportation Research Board (TRB). British Maritime Technology*, vol. 20, nº Feb., pp. 14-24, 1995.

